JOURNAL OF GEOPHYSICAL RESEARCH, VOL. 100, NO. C9, PAGES 18,271–18,280, SEPTEMBER 15, 1995

Numerical experiments on the effects of a meridional ridge on the transmission of energy by barotropic Rossby waves

R. P. Matano

College of Oceanic and Atmospheric Sciences, Oregon State University, Corvallis

Abstract. Analytical and numerical models are used to study the effects of a meridional ridge on the propagation of barotropic Rossby waves produced by distant wind stress forcing. The analytical model illustrates the qualitative aspects of the problem by solving a simplified form of the potential vorticity equation. The analytical results are complemented by numerical experiments using a shallow-water model. In these experiments, waves are excited near the eastern boundary of the model. The effect that the presence of a meridional ridge has on the propagation of these waves is evaluated using spectral analysis. The numerical experiments show that the ridge acts as a low-pass filter for westward propagating waves. In a 4000-m deep ocean a ridge 500 km wide and 500 m high has little effect in preventing energy transmission by barotropic waves. The topographic effect increases sharply with the ridge's height so that a 2000-m ridge almost isolates two neighboring subbasins. The numerical results indicate that for the range of geophysically relevant cases the ridge's width plays only a minor role.

1. Introduction

In order to understand oceanic variability, it is necessary to understand how the ocean adjusts to changes in the wind stress forcing. Large-scale, low-frequency wind or atmospheric pressure fluctuations can excite free waves in the ocean. These waves, the well-known Rossby waves, exist because of the restoring force provided by latitudinal changes in the Coriolis parameter. If the wind or pressure fluctuations have periods of less than a year, the free waves generated are mostly depth independent, barotropic modes, since the baroclinic waves at these low frequencies have restrictively low phase speeds [*Anderson and Corry,* 1977; *Willebrand et al.*, 1980].

The dominance of barotropic variability in the ocean is supported by a number of observational studies. *Koblinsky and Niiler* [1982] studied the relations between wind and current near Barbados. They found significant coherence between the fluctuations of the trade winds and the meridional ocean currents at periods of less than 2 months. *Dickson et al.* [1982] analyzed current meter data from the eastern North Atlantic and suggested that the observed seasonal changes in eddy kinetic energy were correlated with atmospheric variability. *Luther et al.* [1990] showed that significant coherence can be found between bottom pressure and wind stress curl for periods between 2 and 28 days. The relationship between barotropic oceanic fluctuations and the atmospheric forcing has also been investigated in a series of analytical and numerical studies [e.g., *Frankignoul and Müller,* 1979; *Willebrand et al.*, 1980; *Müller and Frankignoul,* 1981; *Brink,* 1989; *Samelson,* 1990; *Samelson and Shrayer,* 1991; *Cummins,* 1991].

The propagation of barotropic Rossby waves can be strongly influenced by the topography of the ocean floor. Large-scale ridges or seamounts may attenuate barotropic modes at some frequencies. A rough bottom may prevent any wave propagation [*Rhines and Bretherton,* 1973]. For a large-scale feature such as the Mid-Atlantic Ridge, the topographic influence upon the barotropic motion is expected to be of the same order of magnitude as the gradient of planetary potential vorticity (the β effect) that sustains ordinary Rossby waves [*Barnier,* 1984a]. The first research on the effects of bottom topography on the propagation of barotropic Rossby waves is described in the seminal papers by *Rhines* [1969] and *Rhines and Bretherton* [1973]. *Rhines* [1969] analyzed the effects of both a topographic step and a smooth triangular ridge using an analytical model. These topographic features reflected most of the incident energy carried by low-frequency waves. *Rhines and Bretherton* [1973] studied the effects of a rough bottom on the propagation of energy by barotropic waves and found both a strong reduction in the amount of energy that can be transmitted and a shrinking in the scales imposed by the forcing. *Kroll and Niiler* [1976] investigated the transmission of energy by barotropic Rossby waves incident on a continental shelf. According to their results, very little of the energy incident from the open ocean can penetrate into the shelf region.

Paper number 95JC02090.
0148-0227/95/95JC-02090$05.00

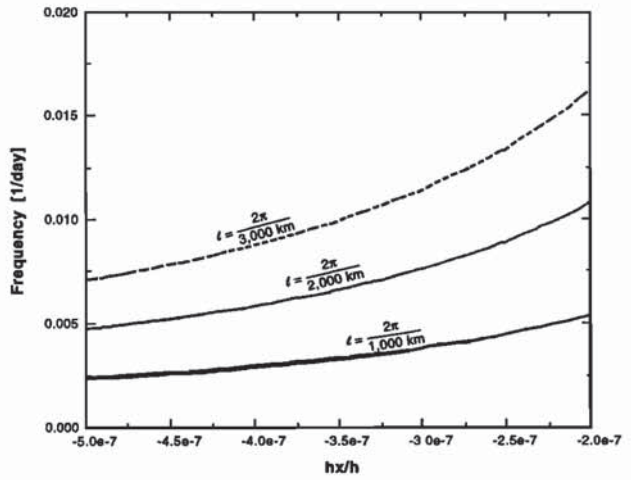

Figure 1. Maximum frequency that is allowed to pass through a topographic barrier without any energy loss as a function of the topography for several values of the meridional wavenumber ℓ.

Anderson and Killworth [1977] studied the effects of a meridional ridge on an ocean basin subjected to a suddenly applied wind stress. For the barotropic case they observed wave reflection along the eastern flank of the ridge. *Barnier* [1984a] studied the transmission properties of eastward propagating waves and found that a topography similar to the Mid-Atlantic Ridge may reflect most of the energy of waves with periods longer than a week. *Barnier* [1984b] investigated the influence of a mid-ocean ridge on the kinetic energy distribution in a midlatitude, barotropic ocean. At periods of 10 days the ocean response to the wind stress forcing consisted of basin-size topographic Rossby modes. At longer periods the response was basin modes relative to the half-basins.

This paper presents new results on how a meridional ridge affects energy transmission by barotropic Rossby waves. Previous studies were based on the results of analytic or semianalytic models that matched plane wave solutions at the boundaries of regions of constant ambient vorticity gradients. A different approach is taken in the first part of this article, where the qualitative effects of a ridge on the wave propagation are studied using perturbation theory. The second part of the present article focuses on the quantitative aspects of the problem using a numerical model that solves the shallow-water equations on a rotating sphere.

2. Theory

The influence of large-scale bottom topography on energy transmission by barotropic Rossby waves has previously been investigated using analytical or semianalytical methods. Solutions to the potential vorticity equation were obtained by matching plane wave solutions at the boundaries of regions of constant ambient vorticity gradients. In these studies the bottom topography was modeled by simple exponential functions. The qualitative effects of more general forms of bottom topography on the propagation of barotropic waves are investigated here using perturbation methods. The bottom topography is represented by a continuous function, and instead of determining energy transmission properties by matching plane wave solutions across slope discontinuities, the evolution of wave packets across changes of topography are calculated using the WKB method.

2.1. Equations

Consider the linear potential vorticity equation for the quasi-geostrophic motion of a homogenous, inviscid fluid [*Rhines*, 1969]

$$\frac{\partial}{\partial t}\left(\nabla^2\psi - \nabla\psi\cdot\frac{\nabla h}{h}\right) + \left(\beta - f\frac{h_y}{h}\right)\frac{\partial\psi}{\partial x} + f\frac{h_x}{h}\frac{\partial\psi}{\partial y} = 0 \qquad (1)$$

where $\psi(x,y,t)$ is the mass stream function, f is the Coriolis parameter, h is the depth of the ocean floor, and β is the meridional gradient of the Coriolis parameter. If ω is a characteristic value of the time derivative, then the ratio of the second to the last term of (1) is of $O[\omega/f]$ and can be neglected for low-frequency waves. This approximation is usually called "Rhines' first approximation." *Veronis* [1966] showed that this simplification is required to avoid the spurious growth associated with the assumption of a constant value for the Coriolis parameter (see *LeBlond and Mysak* [1978] for a more complete discussion on these matters).

Let $h = h(x)$ (analysis of ridges oriented in other directions follows using rotated coordinates). We seek wave solutions of (1) of the form

$$\psi(x,y,t) = \phi(x)h^{1/2}\exp\left[i\left(-\frac{\beta}{2\omega}x + \ell y - \omega t\right)\right] \qquad (2)$$

where ℓ is the meridional wavenumber and ω is frequency. Substituting (2) into (1) gives

$$\frac{d^2\phi}{dx^2} + \kappa^2(x)\phi = 0 \qquad (3)$$

where

$$\kappa^2(x) = \left(\frac{\beta}{2\omega}\right)^2 - \ell^2 - \frac{f\ell}{\omega}\frac{h_x}{h}. \qquad (4)$$

Solutions of (3) depend on the value of the zonal wavenumber $\kappa^2(x)$. If $\kappa^2(x)$ is a positive, slowly varying

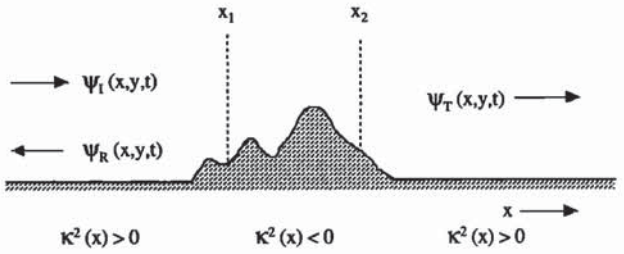

Figure 2. Schematic representation of a flat-bottomed basin divided by a generic meridional ridge.

function, then, in the WKB limit, the only effect of the bottom topography on the wave propagation is a local refraction of the wave packet with no associated loss of energy. If $\kappa^2(x)$ is negative somewhere in the domain, then solutions to (3) decay exponentially and the topography $h(x)$ represents a barrier to energy transmission by propagating waves. The amount of energy that can be transmitted across the ridge depends on the exact form of $h(x)$ and the frequency and direction of the incident waves.

Figure 1 shows the maximum frequency (in the WKB limit) ω_M of waves that may pass over a topographic barrier with no energy loss as a function of both the topographic parameter h_x/h and the meridional wavenumber ℓ. If $\ell \to 0$ (waves traveling in a direction perpendicular to the topographic anomaly), $\omega_M \to \infty$ [*Barnier*, 1984a], which means that there is no frequency restriction by the bottom topography. Since there is no cross-slope motion, the wave does not feel the bottom changes. For a given meridional wavenumber, the maximum frequency decreases with increasing h_x/h (steeper slopes are more effective in reflecting the wave energy).

It has to be noted that the previous discussion applies only in the WKB limit. It is possible, however, to have $\kappa^2 > 0$ everywhere and still have energy losses if there are rapid changes in the bottom slopes. In such cases, wave reflection, and the consequent loss of transmitted energy, is related to the abrupt changes in the bottom topography, a situation that clearly violated the WKB assumption of a slowly varying medium.

2.2. A WKB Solution

Consider now the effects of a meridional ridge on the transmission of energy by barotropic Rossby wave packets. Figure 2 is a schematic representation of a flat-bottomed basin divided by a meridional ridge defined by a continuous, but otherwise unspecified, function $h(x)$. A wave packet incident upon the ridge will find a"potential barrier" in the region where $\kappa^2 < 0$. Part of the incident energy will be reflected at the turning line where $\kappa^2 = 0$, while the remaining wave energy will be transmitted across the potential barrier. To determine how much energy can be transmitted across the ridge by a given wave, it is necessary to solve (3) subject to specified boundary conditions. Although no general solution of (3) is known, an approximate solution can be obtained using the WKB method. The WKB method requires that κ^2 be a slowly varying function of x. Specifically, the wavelength of the incident wave must be smaller than the characteristic horizontal scale of the bottom topography. Since even the relatively short, nondivergent barotropic waves that we are interested in have wavelengths comparable to or greater than the characteristic topographic scale, the formal validity of a WKB solution for the study of realistic topographic features is marginal. In spite of this limitation, the WKB method is known to give surprisingly good results well beyond its range of formal validity (see the discussions on this subject by *Nayfeh* [1973] and *Bender and Orzag* [1978]). Following these experiences and since the method will only be applied to investigate the qualitative effects of the bottom topography on the wave propagation, we will proceed with the WKB. In section 3 the approximate analytical results will be compared against results obtained using numerical methods.

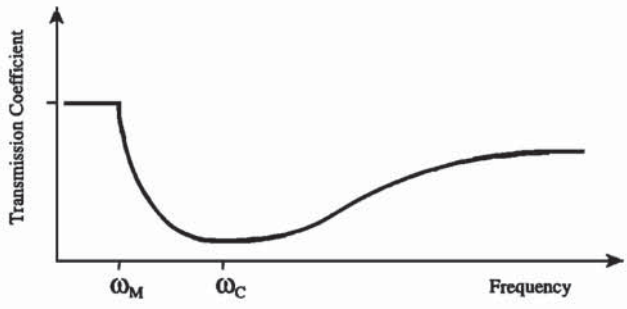

Figure 3. Coefficient of transmission of energy as a function of the frequency for a meridional ridge of Gaussian shape.

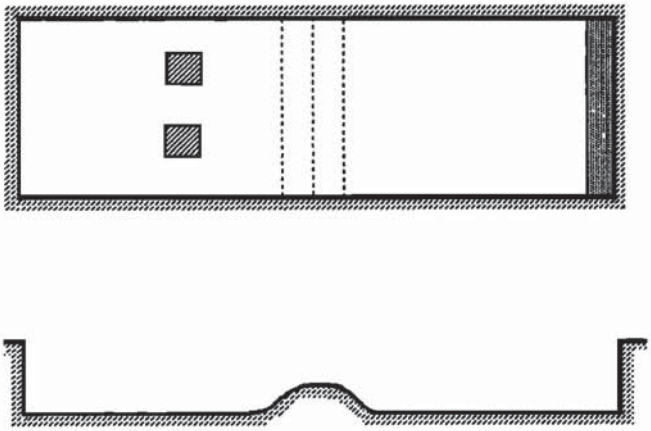

Figure 4. The ocean basin used for the numerical experiments, which is 200° long and 60° wide, with a meridional ridge of Gaussian shape in the middle. The maximum depth is 4000 m. The shadow boxes in the western side of the basin indicate the areas where the energy balances where made. The size of these areas is 10° x 10°. The one to the north is centered at 50°N, and the one to the south is centered at 30°N. The shadow area near the eastern boundary marks the region where the wind stress forcing was applied.

Equation (3) has the WKB solution

$$\phi(x) = A_{\pm} \left[\kappa^2(x)\right]^{-1/4} \exp\left[\pm i \int^x \sqrt{\kappa^2(x)}\, ds\right]. \quad (5)$$

The positive and negative signs yield solutions corresponding to wave packets with eastward or westward group velocity, respectively. *Barnier* [1983] noted that for a given frequency and wavenumber, waves with group velocity in either direction will suffer the same attenuation when crossing over a ridge. It is sufficient therefore to restrict attention to eastward propagating wave packets when elucidating the transmission and reflection coefficients.

Without loss of generality, consider the generic meridional ridge depicted in Figure 2. Then,

$$\kappa^2(x) =< 0 \qquad x_1 < x < x_2$$
$$\kappa^2(x) => 0 \qquad \text{elsewhere}$$

Consider a wave packet incident from the west. The form of the solution for $\phi(x)$ is

$$\begin{aligned}
\phi(x) &= A_I \left[\kappa^2(x)\right]^{-1/4} \exp\left[i\int_x^{x_1} \sqrt{\kappa^2(x)}\, ds\right] \\
&\quad + A_R \left[\kappa^2(x)\right]^{-1/4} \\
&\quad \exp\left[-i\int^{x} \sqrt{\kappa^2(x)}\, ds\right] \qquad x < x_1 \\
\phi(x) &= A_B \left[-\kappa^2(x)\right]^{-1/4} \\
&\quad \exp\left[-\int_{x_1}^{x_2} \sqrt{-\kappa^2(x)}\, ds\right] \qquad x_1 < x < x_2 \\
\phi(x) &= A_T \left[\kappa^2(x)\right]^{-1/4} \\
&\quad \exp\left[i\int_{x_2}^{x} \sqrt{\kappa^2(x)}\, ds\right] \qquad x_2 < x
\end{aligned}$$

where A_I, A_R, and A_T are, respectively, the amplitudes of the incident, reflected, and transmitted waves and A_B is the amplitude of the decay in the region where wave propagation is not possible. Determining the values of these amplitudes is a classical problem in quantum mechanics called "tunneling." Tunneling is a process by which a particle passes through a potential barrier that classical mechanics predicts is impenetrable. Detailed solutions to this problem can be found in textbooks on perturbation theory (e.g., *Nayfeh* [1973] or *Bender and Orzag* [1978]) and will not be repeated here. In the regions where $\kappa^2 \neq 0$ the solutions are propagating or evanescent. As the wave approaches either x_1 or x_2, $\kappa^2(x) \to 0$ and the WKB approximation breaks down. One approach used to circumvent this problem is to assume that near the turning lines, $\kappa^2(x) \approx \alpha x$, where α is a constant. Under this assumption, (3) becomes the Airy equation whose solutions are the Airy functions. The asymptotic matching between the Airy functions and the WKB solution in the neighborhood of x_1 and x_2 permits the calculation of A_R, A_B, and A_T as a function of A_I. It is then possible to compute the coefficient of energy transmission T as

$$T = \frac{|A_T|^2}{|A_I|^2} \approx \exp\left\{-\int_{x_1}^{x_2} \sqrt{-\left[\left(\frac{\beta}{2\omega}\right)^2 - \ell^2 - \frac{f\ell}{\omega}\frac{h_x}{h}\right]}\, ds\right\}. \quad (6)$$

Figure 3 shows a schematic representation of the coefficient T as a function of frequency for a meridional ridge with a Gaussian cross section. For waves with frequencies higher than ω_c, T increases with increasing frequency. For this type of wave the wavelength of the incident wave increases with increasing frequency. Longer waves are less affected by the topographic anomaly. For waves with frequency smaller than ω_c, T increases with decreasing frequency. This corresponds to the case of waves with westward group velocity (longer waves have smaller frequencies). The total amount of energy transmitted decreases with the height of the ridge and increases with its width. The numerical values of ω_M and ω_c depend on the characteristics of the bottom topography and the incident wave. For a meridional ridge of 2000-m height, ω_c has an approximate value of 1/60 days^{-1} and decreases with increasing heights. For the case of a ridge with 1000 m height and 500 km width, ω_M has a value close to 1/150 days^{-1}. This value decreases with the height of the ridge and increases with the meridional wavenumber of the incident wave. For realistic topographic scales the predicted amount of energy that can be transmitted is negligible for waves with frequencies higher than ω_M, which implies that the most important effect of a meridional ridge on the westward propagation of barotropic waves is to act as a filter of high frequencies.

3. Numerical Experiments

The analytical solution to the potential vorticity equation described section 2.2 illustrates the qualitative effects of a meridional ridge on the transmission of energy by barotropic Rossby waves. The approximations required to derive (6) prohibits quantitative evaluations. In this section a numerical model is used to confirm the qualitative results derived in section 2 and to extend these results to quantify the "filtering powder" of ridges of different sizes.

3.1. The Model

The numerical model used in these experiments solves the barotropic shallow-water equations on a rotating sphere, i.e.,

$$\frac{Du}{Dt} - \left(2\Omega + \frac{u}{R\cos\theta}\right) v\sin\theta = -\frac{g}{R\cos\theta}\frac{\partial\eta}{\partial\lambda} - ru$$

$$\frac{Dv}{Dt} - \left(2\Omega + \frac{u}{R\cos\theta}\right) u\sin\theta = -\frac{g}{R}\frac{\partial\eta}{\partial\theta} - rv$$

$$\frac{\partial\eta}{\partial t} + \frac{1}{R\cos\theta}\left\{\frac{\partial}{\partial\lambda}\left[(\eta + H)\,u\right] + \frac{\partial}{\partial\theta}\left[(\eta + H)v\cos\theta\right]\right\} = 0$$

$$\frac{D}{Dt} = \frac{\partial u}{\partial t} + \frac{u}{R\cos\theta}\frac{\partial}{\partial\lambda} + \frac{v}{R}\frac{\partial}{\partial\theta},$$

where u and v are the zonal and meridional components of velocity, η is the sea surface elevation, λ and θ denote longitude and latitude, $H(x, y)$ is the bottom depth, R is the radius of the Earth and Ω its angular velocity, g is the acceleration of gravity, and r is the coefficient of linear bottom friction.

The numerical scheme used to solve the shallow-water equations follows the enstrophy-conserving, staggered grid formulation proposed by *Sadourney* [1975]. The time integration is done using a leapfrog, centered scheme with time smoothing of all dynamical vari-

ables to avoid mode splitting. The model resolution is 1° and the computational code was developed by R. Pacanowski at the Geophysical Fluid Dynamics Laboratory (Princeton, New Jersey). The model domain (Figure 4) is a rectangular basin 200° long and 60° wide centered at 40°N. The model has a constant depth of 4000 m everywhere except in the middle of the basin, where there is a meridional ridge of Gaussian shape. The basin was chosen to be very long in the zonal direction to avoid the interactions between the regions where the forcing is applied and the neighborhood of the ridge. The large meridional extent allows comparison between results from high and low latitudes.

To create westward propagating waves, the model was forced near the eastern boundary with a wind stress of the form

$$\tau = \tau_0 \exp\left\{-\frac{(x - x_{\text{East}})^2}{\Delta^2}\right\} F(t) \tag{7}$$

x and y denote respectively zonal and meridional coordinates, $\tau_0 = 0.1$ N m^{-2}, and $\Delta = 500$ km. The function $F(t)$ defines the time dependence of the wind stress forcing, and it will be discussed later.

The wind stress acts on a relatively small area near the eastern boundary, where it creates a forced response. At the coastal boundary, free Rossby waves cancel the normal component of the forced flow. These waves then propagate away from the forcing area and travel westward as free waves. To avoid spurious energy propagation by coastal Kelvin waves near the northern and southern boundaries of the model, the coefficient of bottom friction was increased using a hyperbolic tangent function from its value of $1/200$ days^{-1} in the open ocean to $1/2$ days^{-1} near the walls. The same procedure was used near the western boundary of the basin to avoid the reflection of short, eastward propagating Rossby waves.

3.2. The Experiments

Two series of experiments were conducted. The first is a qualitative study on the effects of a meridional ridge on the propagation of planetary waves when the wind forcing is modulated in time by a single harmonic component. In the second series of experiments the forcing was modulated in time by a stochastically generated function with prescribed spectral properties. The effect of the height and width of the ridge on the energy transmission was quantified using spectral analysis.

In the first experiment the wind stress forcing is modulated in time by a cosine function with a period of 1 month. The height of the ridge is 1000 m and its e-folding width is 500 km. Figure 5 (top and bottom) shows the time-longitude plots of the free surface elevation for slices taken along 50°N and 20°N, respectively. In Figure 5 the westward propagation of the waves is evident from the negative slopes of the contours. Near the ridge, part of the incident energy is reflected by short waves with eastward group velocity. This reflection is evidenced in Figure 5 (top and bottom) by the wiggling contours to the east of 100°. Part of the energy incident over the ridge is trapped as topographic waves. These waves travel in the meridional direction and are dissipated near the top and bottom boundaries of the model by the increased bottom friction in those areas. The remaining incident energy continues propagating to the west. A comparison between the two panels of Figure 5 shows that the effects of the ridge are more pronounced at high latitudes. Note that at 20°N the amplitudes of the sea surface elevation are quite similar on both sides of the ridge. At 50°N, however, the amplitudes to the east of the ridge are almost twice as large as those in the western part of the basin. This latitudinal effect can be explained by considering the potential vorticity equation for the sea surface elevation,

$$\frac{\partial}{\partial t}\left[\frac{1}{H}\nabla\cdot(H\nabla\eta) - \frac{f^2}{gH}\eta\right] + J(\eta, f) - \frac{f}{H}J(\eta, H) = 0 \tag{8}$$

The first term of (8) is the time rate of change of relative vorticity, the second term represents the change in planetary vorticity, and the last term is the change in vorticity due to the stretching of the water columns by the variation of the bottom topography. The relative importance of the topography can be estimated from the ratio of the second and third terms of (8), namely,

$$\frac{fJ(\eta, H)}{HJ(\eta, f)} \approx O\left(\frac{\alpha \tan\theta}{H_0}\right), \tag{9}$$

where α is a scale parameter for the topographic slope, and H_0 is the mean water depth. For large values of the ratio (9) the vorticity balance is dominated by the topographic term and the β effect can be neglected. For small values of this ratio the effects of bottom topography are negligible and the dynamics are those of pure Rossby waves in a flat-bottomed ocean. For a given bottom topography, (9) changes with latitude because of changes in both f and β. At low latitudes the higher values of β and the lower values of f combine to reduce the importance of bottom topography. Topographic control should therefore increase with latitude, as observed.

This experiment gives a qualitative picture of the effects of a meridional ridge on the propagation of barotropic Rossby waves. It is desirable, however, to quantify the topographic effect on waves of different frequencies and therefore of different wavelengths. To this end, waves of a broad range of frequencies were excited at the eastern side of the basin using a stochastic wind forcing. To analyze the effects of a meridional ridge on the wave propagation, a reference experiment was run in a flat-bottomed basin and spectral analysis of energy budgets were done at selected locations. A meridional ridge was then included, and the energy balances repeated. The comparison between the energy spectra allows an assessment of the quantitative and qualitative effects of bottom topography on the energy transmission by barotropic Rossby waves.

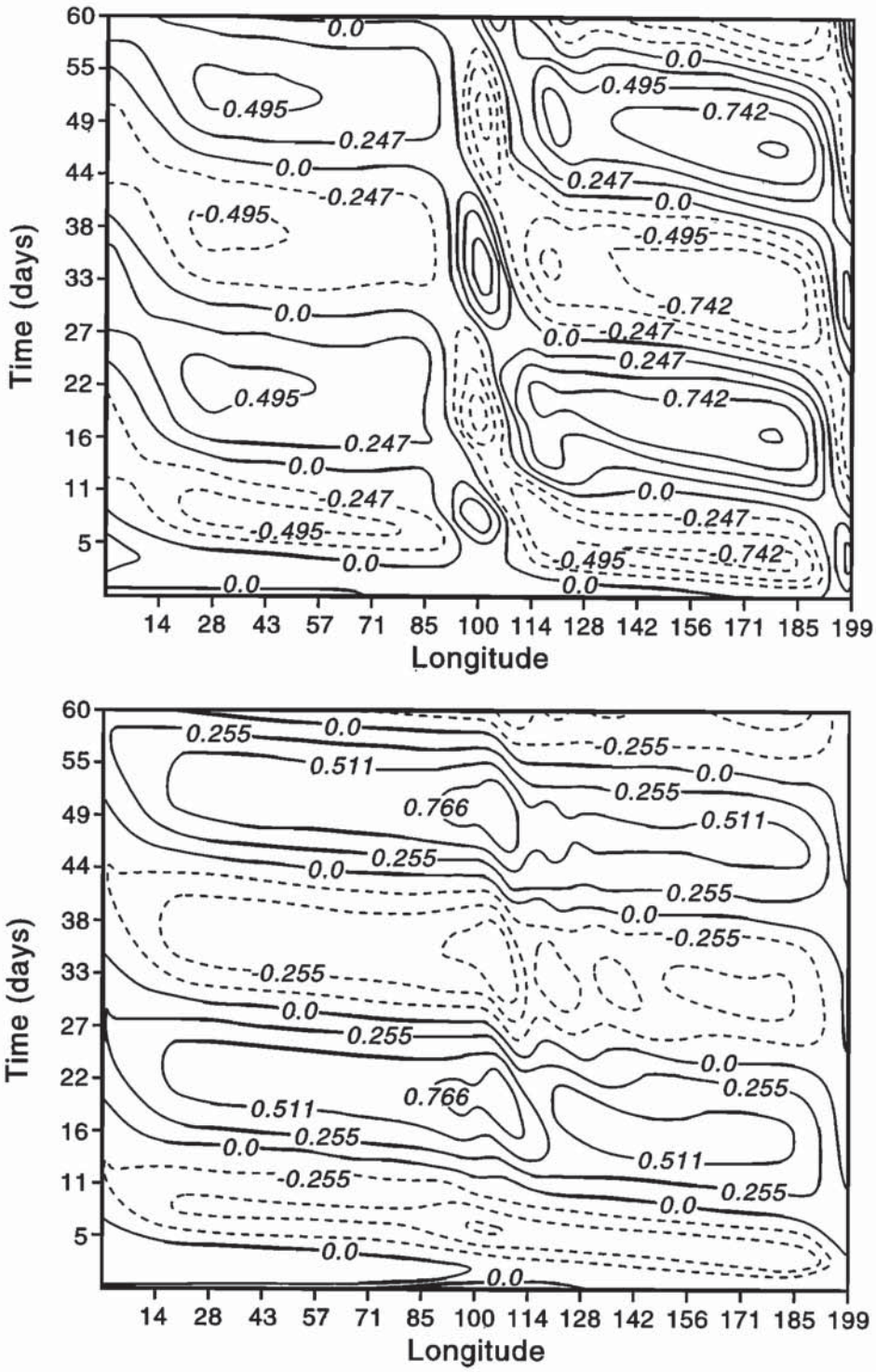

Figure 5. Time-longitude plots of the free surface elevation of the numerical model taken along (top) 50°N and (bottom) 20°N.

To generate westward propagating waves, the model was forced with a wind stress of specified spectral characteristics. Figure 6 shows the chosen wind stress power spectra; it is white for periods longer than a few days and decreases exponentially for higher frequencies. The time series associated with this power spectra (function $F(t)$ in (7)) was calculated using a discrete Fourier transform, and these values were interpolated to the time steps of the model using a cubic spline. The model was then started from rest and run for 10 years using the stochastic forcing.

Figure 7 shows snapshots of the sea surface elevation. Figure 7 (top) shows the case of a flat-bottomed basin, while the two middle and bottom panels correspond to the case of a basin divided by a meridional ridge 1000 m high. For the case of a flat-bottomed basin the sea

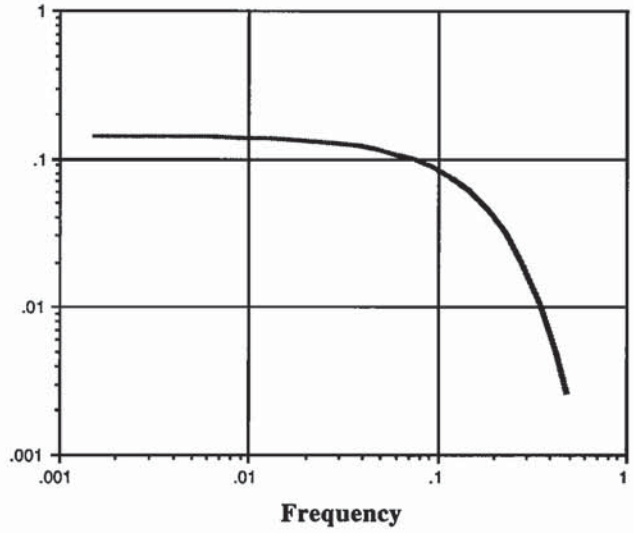

surface elevation map is dominated by long-scale features everywhere except the western boundary. When a meridional ridge is included, there are marked differences between the dominant scales at the two sides of the ridge. While to the west of the ridge, the sea surface elevation is mostly dominated by long-scale features, there are sea level disturbances of several scales to the east of the ridge. The effect of the ridge is to act as a filter for short-scale disturbances, which are mostly reflected as eastward propagating Rossby waves, that give its distinct appearance to the eastern side of the basin.

Figure 6. Energy spectra of the wind stress forcing. The time series associated with this spectra was calculated using a discrete Fourier transform, and these values were then interpolated into the time steps of the model using a cubic spline.

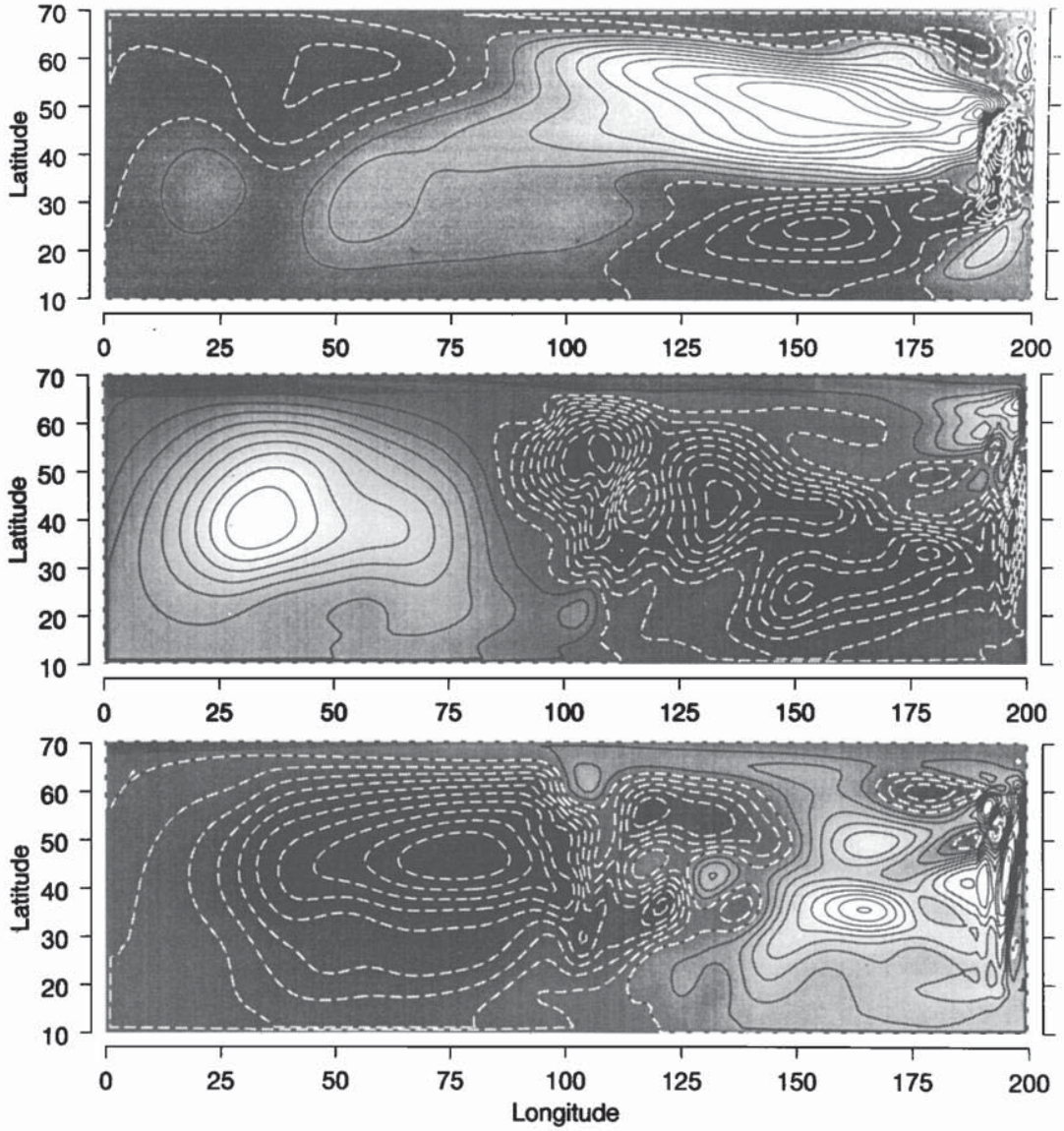

Figure 7. Snapshots of the sea surface elevation at days 300, 330, and 360 of two numerical simulations, (top) for a flat-bottomed basin for a basin that has a meridional ridge (middle) 500 km wide and (bottom) 1000 m high. The contour interval is 0.1 m, and dashed lines represent negative values.

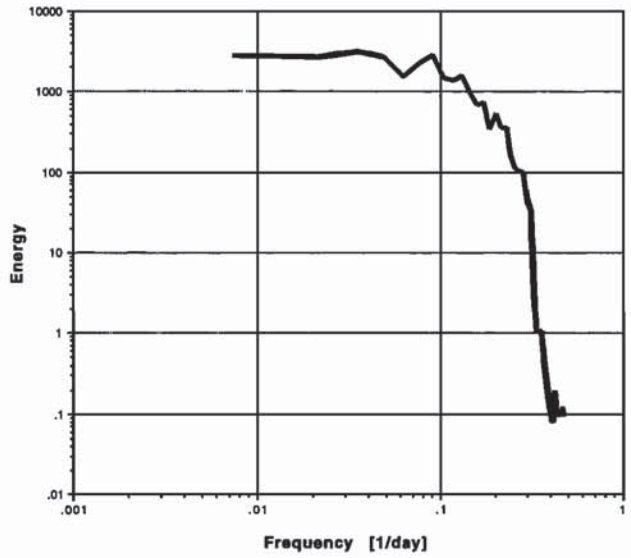

Figure 8. Power spectra of the total energy in the low-latitude area of the model for a flat-bottomed basin. The corresponding spectra for the high-latitude region are qualitatively similar.

To quantify the amount of energy that is allowed to cross a given ridge, the kinetic energy of the model was calculated in the shaded areas of Figure 4. A coefficient of energy transmission was defined as

$$T_E(\omega) = \frac{S(\omega)}{S_0(\omega)}$$

where $S(\omega)$ is the amount of energy in the area when a ridge is present and $S_0(\omega)$ is the amount of energy in the same area for a flat-bottomed basin. Figure 8 shows the power spectra of the total energy in the low-latitude area of the model for the case of a flat-bottomed basin.

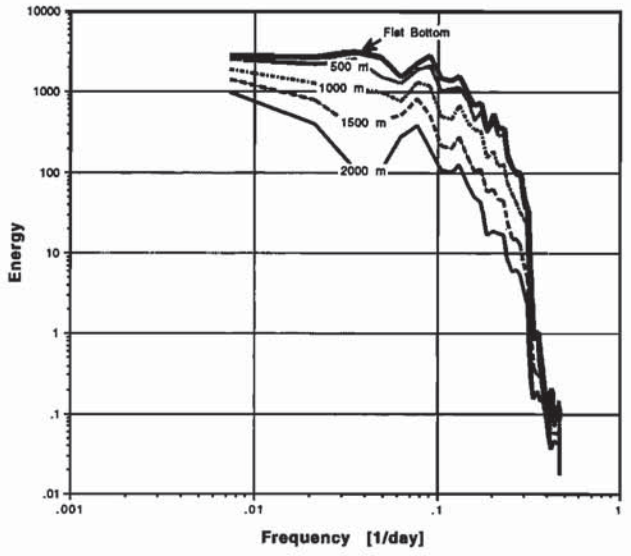

Figure 9. Energy spectra in the low-latitude region for a flat-bottomed ocean and for basins with ridges of 500, 1000, 1500, and 2000 m. The ridge's width was 500 km in all cases.

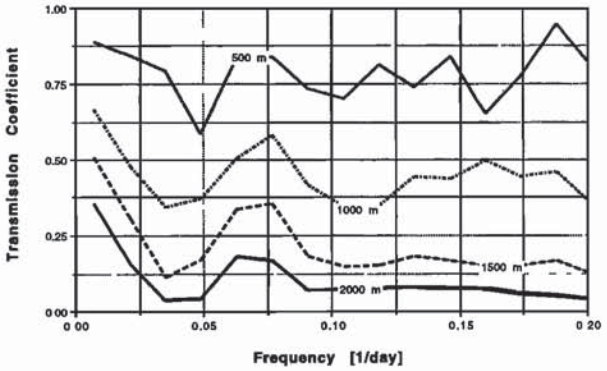

Figure 10. Transmission coefficients in the low-latitude area of the basin.

The spectra in the high-latitude region are qualitatively similar. Like the wind stress, the oceanic spectra have most of its energy concentrated in the low frequencies. The peaks observed in the neighborhood of 10 days are associated with the resonant excitation of basin modes, i.e.,

$$T = 4\pi^2 \frac{\sqrt{\frac{m^2}{L_x^2} + \frac{n^2}{L_y^2}}}{\beta},$$

where T is the period of the n, m mode and L_x and L_y are the dimensions of the basin [*Pedlosky*, 1987].

Figure 9 shows the energy spectra calculated in the low-latitude area for a flat-bottomed basin and for ridges with heights of 500, 1000, 1500, and 2000 m. The ridge width was 500 km in all cases. The peaks of the transmission coefficient for periods between 10 and 20 days are related to the shifting of the resonant modes by the bottom topography. Although a 500-m ridge does not strongly affect the westward energy propagation, increasing the ridge height has a marked effect in the amount of energy that is allowed to pass from the

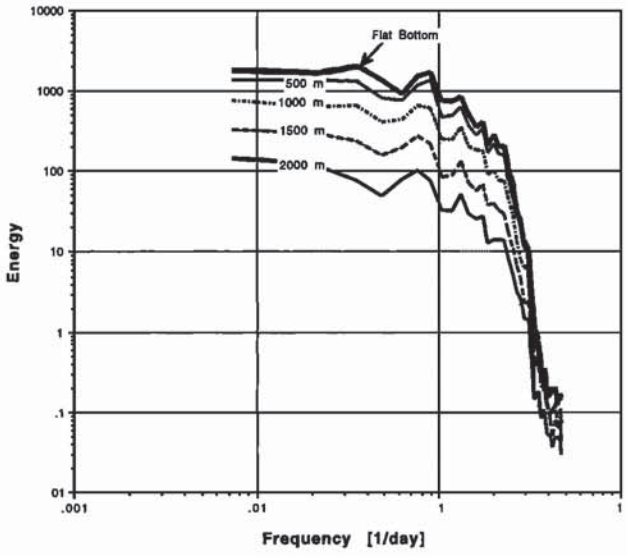

Figure 11. Same as Figure 9, but for the high-latitude region.

eastern to the western side of the basin. The energy transmitted is substantially reduced, and the resulting energy spectra become noticeably redder. Figure 10 shows the transmission coefficients calculated for these cases. For waves with periods smaller than a month the transmission coefficient remains approximately constant. There is a strong reduction in the energy transmitted when the ridge height is increased. While a 500-m ridge will pass approximately 90% of the incident energy, a 2000-m ridge will pass less than 10%.

The qualitative characteristic of the results is in agreement with those predicted from the WKB model. Estimates of the frequency ω_c (see Figure 3) for different values of the meridional wavenumber gave values between 1/10 and 1/60 days^{-1}. For a ridge of 1000 m height and 500 km width the parameter $h_x/h \approx 5.10^{-7}$; for waves with a meridional wavelength of 3000 km the analytical model of the previous section (see Figure 1) predicts that only waves with periods greater than 5 months would pass with no energy attenuation. If the meridional wavelength is reduced to 1000 km (a value more characteristic of midlatitude storms), then the minimum period increases to a value longer than a year.

Figures 11 and 12 show the spectra and the energy transmission coefficient for the high-latitude area. As noted before, at high latitudes the topographic barrier is more effective in preventing westward energy transmission. This effect is easily discernible for ridges lower than 1000 m. For higher ridges the amount of energy transmitted is insignificant at high as well as low latitudes. It should be noted that the present definitions of "high" and "low" latitudes do not encompass the broad range of latitudes that is usually associated with these terms. In the present context the term low latitudes refers to areas around 30° (and not equatorial regions), while the term high latitudes refers to areas around 50°. The latitudinal effects would have been more accentuated had we chosen more extreme regions to make our calculations, but at higher or lower latitudes the relevance of barotropic waves in the oceanic adjustment diminishes, making the problem less relevant.

Another series of experiments were conducted to check the effect of the ridge width on the wave propagation. To that end, the ridge width was increased from 500 to 1000 km and then decreased to 200 km. The results of those experiments are not shown because they are not substantially different to those just described. The general outcome is that a wider ridge favors the wave passage through the topographic barrier. For the geophysically relevant case, such effect is very small in comparison to those associated with changes in the ridge height.

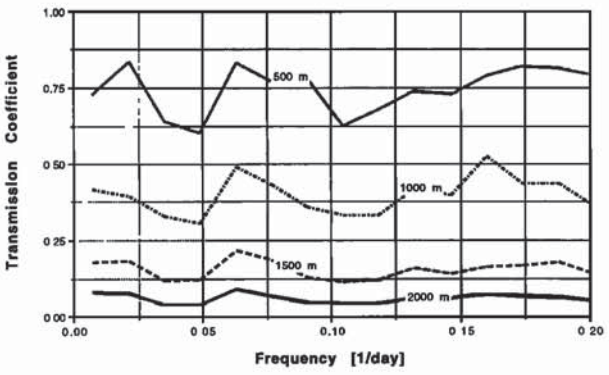

Figure 12. Same as Figure 10, but for the high-latitude region.

4. Summary and Discussion

We have used analytical and numerical models to study the properties of energy transmission by barotropic Rossby waves across a meridional ridge. The analytical model obeys a simplified form of the barotropic potential vorticity equation that is solved by the WKB method. For the most relevant case of westward propagating waves, energy transmission across the ridge is enhanced for long-period waves (larger wavelength). Although the analytical solution clarifies the qualitative properties of the energy transmission, it is not adequate for quantitative analysis because of the approximations involved in its derivation. For quantitative purposes we have used a numerical model that solves the discrete form of the primitive equations on a rotating sphere. The numerical experiments indicate that a meridional ridge acts as a low-pass filter for westward propagating waves. In a 4000-m deep ocean a ridge 500 km wide and 500 m high has little effect in preventing energy transmission by barotropic waves. The topographic effect increases sharply with the ridge's height so that a 2000-m ridge almost isolates two neighboring subbasins. The numerical results indicate that for the range of geophysically relevant cases the ridge's width plays only a minor role in the attenuation of propagating waves.

It has long been argued [*Gill and Niiler,* 1973; *Anderson and Corry,* 1977; *Willebrand et al.,* 1980] that the oceanic adjustment to seasonal wind changes is accomplished primarily by the propagation of barotropic Rossby waves. It is important to understand how the propagation of these waves is affected by the underlying bottom topography. The case presented here and those previously studied by other authors are steps in that direction. The fact that a meridional ridge will act as a low-pass filter for high-frequency fluctuations may explain why western boundary currents such as the Gulf Stream [*Anderson and Corry,* 1977; *Greatbatch and Goulding,* 1989] or the Brazil Current may have seasonal cycles that can be directly related to the low-frequency changes in the wind stress forcing.

It is, of course, obvious that a meridional ridge, a basically one-dimensional problem, is just a first step in the understanding of topographic effects. Its appeal is that direct comparison can be made between numerical and analytical solutions. For a more realistic approach, however, two-dimensional topography and the effect of density stratification should be included. The barotropic problem with a two-dimensional topography can be interpreted in terms of basin modes

and "teleconnections" between them. The fully three-dimensional problem, however, requires consideration between barotropic and baroclinic interactions, which makes the problem far more complicated. By the time this manuscript was completed we became aware of a recent analytical study by *Wang and Koblinsky* [1994] that investigates the interaction between barotropic and baroclinic modes forced by a meridional ridge.

Acknowledgments. This article benefited from the comments of two anonymous reviewers. This research was support by contract 958127 from the Jet Propulsion Laboratory funder under the TOPEX Announcement of Opportunity. The modeling was carried out on the Cray Y-MP8/864 computer at the NASA Center for Computational Sciences at Goddard Space Flight Center under funding from NASA grant NAGW-3510.

References

Anderson, D. L. T., and R. A. Corry, Ocean response to low frequency forcing with application to the seasonal variations in the Florida Straits-Gulf Stream Transports, *Prog. Oceanogr., 14,* 7–40, 1977.

Anderson, D. L. T., and P. D. Killworth, Spin-up of a stratified ocean with topography, *Deep Sea Res., 24,* 709–732, 1977.

Barnier, B., Energy transmission by barotropic Rossby waves across large-scale topography, *J. Phys. Oceanogr., 14,* 438–447, 1984a.

Barnier, B., Influence of a mid-ocean ridge on wind-driven barotropic Rossby waves, *J. Phys. Oceanogr., 14,* 1930–1936, 1984b.

Bender, C. M., and S. A. Orzag, *Advanced Mathematical Methods for Scientists and Engineers,* McGraw-Hill, New York, 1978.

Brink, K. H., Evidence for wind-driven current fluctuations in the western North Atlantic, *J. Geophys Res., 94,* 2029–2044, 1989.

Cummins, P. F., The barotropic response of the subpolar North Pacific to stochostic wind forcing, *J. Geophys. Res., 96,* 8869–8880, 1991.

Dickson, R. R., W. J. Gould, P. A. Gurbutt, and P. P. Killworth, A seasonal signal in the ocean currents to abyssal depths, *Nature, 295,* 193–198, 1982.

Frankignoul, C., and P. Müller, Quasigeostrophic response on an infinite β-plane ocean to stochastic forcing by the atmosphere, *J. Phys. Oceanogr., 9,* 104–127, 1979.

Gill, A. E., and P. P. Niiler, The theory of the seasonal variability in the ocean, *Deep Sea Res., 20,* 141–177, 1973.

Greatbatch, R. J., and A. Goulding, Seasonal variations in a linear barotropic model of the North Atlantic driven by the Hellerman and Rosenstein wind field, *J. Phys. Oceanogr., 19,* 572–595, 1989.

Koblinsky, C. J., and P. P. Niiler, The relationship between deep ocean currents and winds east of Barbados, *J. Phys. Oceanogr., 13,* 1093–1104, 1982.

Kroll, J., and P. P. Niiler, The transmission and decay of barotropic Rossby waves incident on a continental shelf, *J. Phys. Oceanogr., 6,* 432–450, 1976.

LeBlond, P. H., and L. A. Mysak, *Waves in the Ocean, Elsevier Oceanogr. Ser.,* Elsevier, New York, 1978.

Luther, D. S., A. D. Chave, J. H. Filloux, and P. F. Spain, Evidence for local and nonlocal barotropic responses to atmospheric forcing during BEMPEX, *Geophys. Res. Lett., 17,* 949–952, 1990.

Müller, P., and C. Frankignoul, Direct atmospheric forcing of geostrophic eddies, *J. Phys. Oceanogr., 11,* 287–308, 1981.

Nayfeh, A. H., *Perturbation Methods,* John Wiley, New York, 1973.

Pedlosky, J., *Geophysical Fluid Dynamics,* 2nd ed., 710 pp., Springer-Verlag, New York, 1987.

Rhines, P. B., Slow oscillations in an ocean of varying depth, I, Abrupt topography, *J. Fluid Mech., 37,* 161–189, 1969.

Rhines, P. B., and F. Bretherton, Topographic Rossby waves in a rough-bottomed ocean, *J. Fluid Mech., 61,* 538–607, 1973.

Sadourney, R., The dynamics of finite-difference models of the shallow-water equations, *J. Atmos. Sci., 32,* 680–689, 1975.

Samelson, R. M., Evidence for wind-driven current fluctuations in the eastern North Atlantic, *J. Geophys. Res., 95,* 11,359–11,368, 1990.

Samelson, R. M., and B. Shrayer, Currents forced by stochastic winds with meridionally varying amplitude, *J. Geophys. Res., 96,* 13,452–13,463, 1991.

Veronis, G., Rossby waves with bottom topography, *J. Mar. Res., 24,* 338- 349, 1966.

Wang, L., and C. J. Koblinsky, Influence of mid-ocean ridges on Rossby waves, *J. Geophys. Res., 99,* 25,143–25,153, 1994.

Willebrand, J. S., S. G. H. Philander, and R. C. Pacanowski, The oceanic response to large scale atmospheric disturbances, *J. Phys. Oceanogr., 10,* 411–429, 1980.

R. P. Matano, College of Oceanic and Atmospheric Sciences, Oregon State University, Oceanography Administration Building 104, Corvallis, OR 97331-5503. (e-mail: rpm@oce.orst.edu)

(Received July 28, 1994; revised May 1, 1995;
accepted June 29, 1995.)